Thermoelectric power of graphene as surface charge doping indicator

Anton N. Sidorov,[1,a)] Andriy Sherehiy,[2] Ruwantha Jayasinghe,[2] Robert Stallard,[2] Daniel K. Benjamin,[1] Qingkai Yu,[3] Zhihong Liu,[3] Wei Wu,[4] Helin Cao,[5] Yong P. Chen,[5] Zhigang Jiang,[1,b)] and Gamini U. Sumanasekera[2,c)]
[1]*School of Physics, Georgia Institute of Technology, Atlanta, Georgia 30332, USA*
[2]*Department of Physics, University of Louisville, Louisville, Kentucky 40292, USA*
[3]*Ingram School of Engineering and Materials Science, Engineering and Commercialization Program, Texas State University, San Marcos, Texas 78666, USA*
[4]*Center for Advanced Materials and Department of Electrical and Computer Engineering, University of Houston, Houston, Texas 77204, USA*
[5]*Department of Physics, Purdue University, West Lafayette, Indiana 47907, USA*

(Received 18 April 2011; accepted 10 June 2011; published online 8 July 2011)

We report on simultaneous thermoelectric power and four-probe resistance measurements of chemical vapor deposition grown graphene during a degas process, as well as in exposure to various gases. For all investigated samples, a dramatic change in thermoelectric power was observed and found to be sensitive to the gas molecule charge doping on the surface of graphene. The observed p-type behavior under ambient conditions supports an electrochemical charge transfer mechanism between the graphene and oxygen redox couple, while the n-type behavior under degassed conditions is ascribed to the electron doping caused by the surface states of the SiO_2/Si substrate. © *2011 American Institute of Physics*. [doi:10.1063/1.3609858]

Recently, graphene has emerged as a candidate material of great interest for next generation nanoelectronics. Physical properties of graphene have already been explored; fascinating electrical, thermal, optical, and mechanical characteristics have been found well integrated in this intriguing material. Compared with conventional two-dimensional semiconductor systems, such as heterostructures or quantum wells, graphene proves to be more sensitive to its environment, i.e., the supporting substrate and gases/chemicals adsorbed on the surface.[1–3] Annealing graphene in high vacuum or with a H_2-Ar gas mixture has long been recognized as a key process to improve the device quality.[4,5] In this letter, we present a comparison study of the response of the thermoelectric power (TEP) and the four-probe resistance of graphene during vacuum annealing and in exposure to various gases. We demonstrate that TEP is a more sensitive measure of surface charge doping on graphene, holding promise for practical applications such as thermoelectric gas sensors.

The graphene specimens (monolayers) utilized in this work were synthesized by the chemical vapor deposition (CVD) method at ambient pressure on polycrystalline Cu foils and then transferred onto SiO_2/Si substrates, as described in Ref. 6. Availability of large-area CVD-grown graphene[6,7] facilitates straightforward TEP measurement by anchoring two miniature thermocouples (Chromel-Alumel, K-type) and a resistive heater on the graphene without undergoing any micro-fabrication processes.[8] Use of two extra wires, as current leads, can be easily implemented to measure the four-probe resistance of the device simultaneously.[9] The measured Seebeck coefficient (S) and the four-probe resistance (R) provide complementary information about CVD-grown graphene. In particular, S is very sensitive to the particle-hole asymmetry in graphene, which advances the TEP measurement as a valuable probe to investigate the adsorption mechanism of reactive gases on graphene's surface.

Figure 1 shows the concomitant time evolution of S and R of a CVD-grown graphene device during vacuum annealing with a base pressure below 10^{-6} Torr. Initially, S increases gradually with temperature (T) following the characteristic temperature dependence of the TEP.[10–12] At 400-500 K, however, it undergoes a drastic drop, even with a reversal of sign, and attains a negative value ~ -50 μV/K, while T is set to 500 K. When the sample is cooled back down to room temperature, S increases and eventually saturates at -32 μV/K. During this annealing process, resistance ($R_{starting} \approx 3.7$ kΩ at room temperature) first increases with T, reaches a peak value of 5.4 kΩ, and then drops to 2.3 kΩ when T is stabilized at 500 K. Upon cooling, R decreases further, saturating at 2.0 kΩ. Note that the total percentage change of S is about two times larger than that of R during annealing, indicating its high sensitivity to surface absorption of gas molecules.

Our observation unambiguously shows that under ambient conditions, the Fermi energy level (E_F) of graphene is located in the valence band, giving rise to p-type ($S > 0$) behavior with holes as majority carriers. During degassing, the hole carrier density of states depletes and E_F starts to rise (S decreases and R increases), until E_F crosses the charge neutrality point of graphene, where $S = 0$ and R reaches the Dirac peak (shown in Fig. 1(c)). E_F continues to rise after the transition of the conduction from holes to electrons, and the accumulation of electron carriers is evident from negatively increasing S and decreasing R. For all investigated samples, graphene becomes n-type after vacuum annealing.

The p-type behavior (at ambient) of carbon nanostructures, including single(multi)-walled nanotubes (SWNTs and MWNTs) and activated carbon fibers, has been a topic of

a)Electronic mail: asidorov3@mail.gatech.edu.
b)Electronic mail: zhigang.jiang@physics.gatech.edu.
c)Electronic mail: gusuma01@louisville.edu.

0003-6951/2011/99(1)/013115/3/$30.00 © 2011 American Institute of Physics

Downloaded 08 Jul 2011 to 128.211.161.17. Redistribution subject to AIP license or copyright; see http://apl.aip.org/about/rights_and_permissions

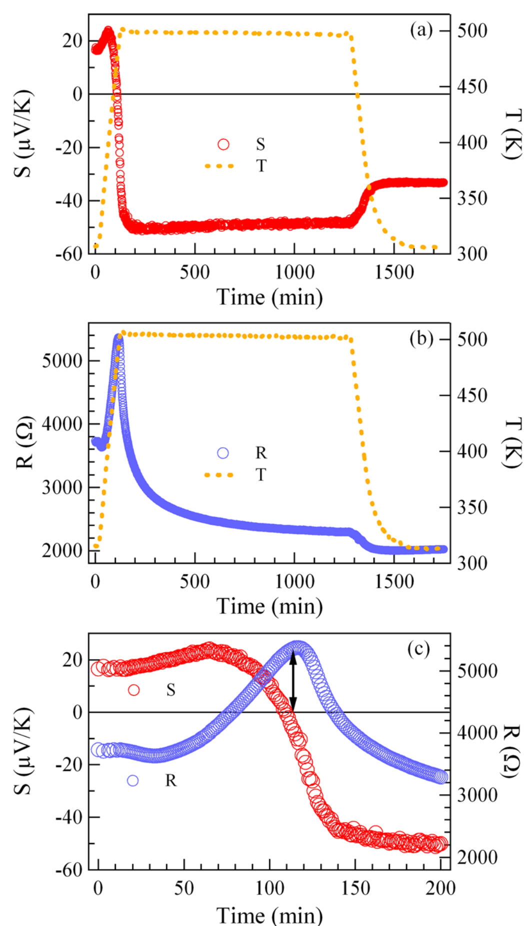

FIG. 1. (Color online) The concomitant time evolution of (a) S and (b) R (red and blue circles – plotted on the left axis) and the corresponding temperature profile (orange dotted lines – plotted on the right axis) of a CVD-grown graphene sample during vacuum annealing. (c) The time evolution of concomitant S and R during the degassing in a blown-up scale.

debate due to various interpretations.[13,14] In the present work, it can be explained as the consequence of electrochemically mediated charge transfer from graphene to the oxygen redox couple in an adsorbed water layer. Recently, a similar charge transfer mechanism has been employed to interpret the E_F pinning in hydrogen-terminated diamond[15–17] and in graphene,[18] affirming that it is a general phenomenon which may influence the properties of semiconductors when the band lineup between the ambient and electronic states in the semiconductor is appropriate.[17] Specifically, as shown in Fig. 2(a), the redox potential of oxygen lies between −5.66 and −4.83 eV with respect to the vacuum level, depending on the pH value of the solution (0 to 14, respectively).[15] This energy range is markedly below the charge neutrality point of graphene, given that its work function is ~4.6 eV.[19] Therefore, spontaneous electron transfer would occur from the graphene to the mildly acidic oxygen/water layer at ambient, mediated by the redox reaction, $O_2 + 4H^+ + 4e^- = 2H_2O$, resulting in the observed p-type behavior. On the other hand, the n-type behavior of CVD-grown graphene after vacuum annealing is consistent with previous observations on mechanically exfoliated graphene and can be attributed to electron doping caused by the surface states of its SiO_2/Si substrate.[3] As illustrated in Fig. 2(b), the work function of SiO_2 is ~3.03 eV, thus the E_F of vacuum-

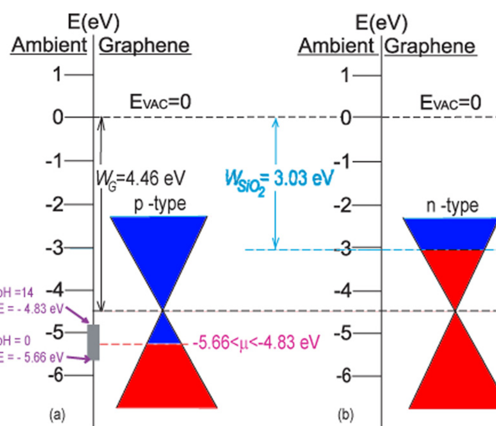

FIG. 2. (Color online) (a) Graphene on a SiO_2/Si substrate is p-type under ambient conditions: E_F is pinned by the redox potential of oxygen dissolved in the mildly acidic water adsorbed on the SiO_2 surface, causing electron transfer from the graphene to the oxygen/water layer. (b) Graphene becomes n-type under degassed conditions: E_F is located in the conduction band due to electron doping by the surface states of the SiO_2/Si substrate.

annealed graphene is expected to be pinned in the conduction band.

The difference in E_F between the graphene at ambient and degassed conditions leads to distinct temperature dependence of S and R before and after vacuum annealing. For oxygen loaded p-type graphene, both S and R increase quadratically during heating (as shown in Fig. 3), suggesting that screened Coulomb scattering by charged impurities may be the dominating scattering mechanism.[20,21] For annealed samples, in which charged impurities due to gaseous species are largely reduced, linear temperature dependence is evident in S and R, and Mott's relation is recovered.[10–12] Specifically, Mott's formula for TEP states that, $S(T) = -\frac{\pi^2}{3|e|}\frac{k_B^2 T}{\sigma(E_F)}\frac{\partial\sigma(E)}{\partial E}|_{E=E_F}$, where e is the electron charge, k_B is Boltzmann's constant, and σ is the conductivity. For the

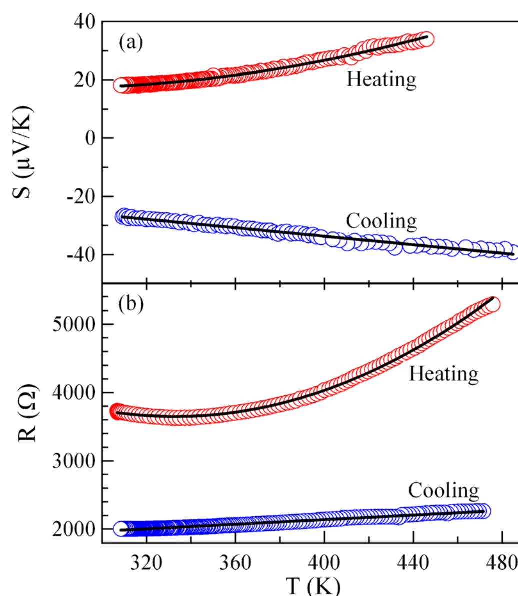

FIG. 3. (Color online) The temperature dependence of (a) S and (b) R of a graphene device during heating (red, prior to the oxygen desorption) and cooling (blue, after degassing). Solid black lines are the fits for quadratic (heating) and linear (cooling) dependences. The data during desorption are excluded in both plots.

Downloaded 08 Jul 2011 to 128.211.161.17. Redistribution subject to AIP license or copyright; see http://apl.aip.org/about/rights_and_permissions

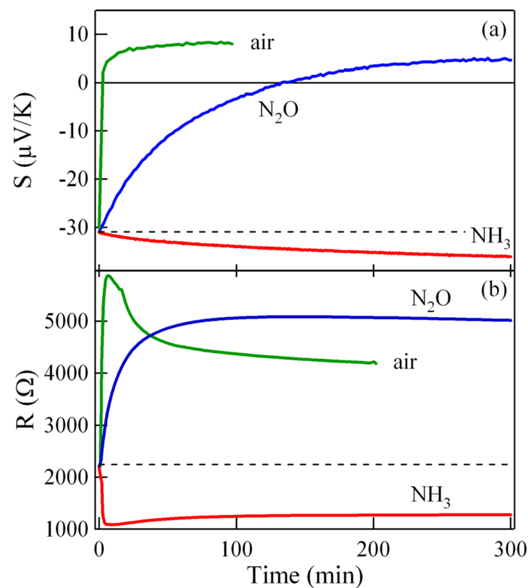

FIG. 4. (Color online) The concomitant time evolution of (a) S and (b) R of CVD-grown graphene upon exposure to air, N_2O, and NH_3. After each exposure, the sample was degassed to recover the original values of S and R before the subsequent exposure.

energy dependent relaxation time, $\tau \propto E^m$, TEP becomes $S(T) = -\frac{\pi^2}{3|e|}\frac{k_B^2 T}{E_F}(m+1)$, where different values of m correspond to different scattering mechanisms, and m only has weak temperature and density dependence.[21]

The high sensitivity of the TEP of graphene to surface charge doping is further demonstrated in Fig. 4, where the device is exposed to air, N_2O, and NH_3. In this study, we start with a fully degassed graphene sample, i.e., initially n-type ($S = -32$ μV/K). Upon exposure, it becomes either p-doped (for air and N_2O) or further n-doped (for NH_3), depending on the properties of the gaseous species. For example, the exposure to N_2O converts graphene to p-type, evidenced by the change in the sign of S (Fig. 4(a)) and the appearance of a maximum in R (Fig. 4(b)), but with a slower rate compared to exposure to the ambient air. N_2O acts as an electron acceptor for graphene, while NH_3 acts as a weak electron donor, consistent to previous studies on SWNTs.[22] Recently, the absorption of N_2O and NH_3 on graphene has been calculated numerically,[23] and the strength of the charge transfer from/to graphene is found to be $-0.099e$ and $0.027e$, respectively, in qualitative agreement with the magnitude change in TEP in our experiment. Note that the change in S is *monotonic* during the exposure, but non-monotonic for R (increase or decrease in resistance depending on the type of the dominating carriers), and therefore S is a better choice of a charge doping indicator. Finally, we stress that the initial degassed state can be recovered after gas exposure by repeating the vacuum annealing process described above to 500 K. Repetitive exposure–annealing cycles have shown no "poisoning" effects of the introduced gases to the graphene devices.

In conclusion, we show that the TEP of CVD-grown graphene is a sensitive probe to the surface charge doping from the environment. Compared with conventional conductometric methods, the thermoelectric sensing paradigm demonstrated herein has the following unique advantages, in addition to its high performance: (1) powered by heat, free energy in electronic systems; (2) associated with intrinsic material properties instead of contact-related properties due to the absence of excitation current; and (3) provides easy means of multiplexed sensing by eliminating multiple current sources and detection interferences. This device concept might be of practical importance in gas/chemical sensing.

This work is supported by the SRC-NRI-MIND and the NSF (Grant Nos. ECCS-0925835 and DMR-0820382). Z.J. acknowledges support from 3M Company.

[1] F. Schedin, A. K. Geim, S. V. Morozov, E. W. Hill, P. Blake, M. I. Katsnelson, and K. S. Novoselov, Nature Mater. **6**, 652 (2007).
[2] T. Lohmann, K. von Klitzing, and J. H. Smet, Nano Lett. **9**, 1973 (2009).
[3] H. E. Romero, N. Shen, P. Joshi, H. R. Gutierrez, S. A. Tadigadapa, J. O. Sofo, and P. C. Eklund, ACS Nano **2**, 2037 (2008).
[4] J. H. Chen, C. Jang, S. D. Xiao, M. Ishigami, and M. S. Fuhrer, Nat. Nanotechnol. **3**, 206 (2008).
[5] S. V. Morozov, K. S. Novoselov, M. I. Katsnelson, F. Schedin, D. C. Elias, J. A. Jaszczak, and A. K. Geim, Phys. Rev. Lett. **100**, 016602 (2008).
[6] X. S. Li, W. W. Cai, J. H. An, S. Kim, J. Nah, D. X. Yang, R. Piner, A. Velamakanni, I. Jung, E. Tutuc, S. K. Banerjee, L. Colombo, and R. S. Ruoff, Science **324**, 1312 (2009).
[7] H. L. Cao, Q. K. Yu, L. A. Jauregui, J. Tian, W. Wu, Z. Liu, R. Jalilian, D. K. Benjamin, Z. Jiang, J. Bao, S. S. Pei, and Y. P. Chen, Appl. Phys. Lett. **96**, 122106 (2010).
[8] G. U. Sumanasekera, L. Grigorian, and P. C. Eklund, Meas. Sci. Technol. **11**, 273 (2000).
[9] See supplementary material at http://dx.doi.org/10.1063/1.3609858 for measurement details.
[10] Y. M. Zuev, W. Chang, and P. Kim, Phys. Rev. Lett. **102**, 096807 (2009).
[11] P. Wei, W. Bao, Y. Pu, C. N. Lau, and J. Shi, Phys. Rev. Lett. **102**, 166808 (2009).
[12] J. G. Checkelsky and N. P. Ong, Phys. Rev. B **80**, 081413 (2009).
[13] G. U. Sumanasekera, C. K. W. Adu, S. Fang, and P. C. Eklund, Phys. Rev. Lett. **85**, 1096 (2000).
[14] V. Derycke, R. Martel, J. Appenzeller, and P. Avouris, Nano Lett. **1**, 453 (2001).
[15] V. Chakrapani, J. C. Angus, A. B. Anderson, S. D. Wolter, B. R. Stoner, and G. U. Sumanasekera, Science **318**, 1424 (2007).
[16] W. Y. Zhang, J. Ristein, and L. Ley, Phys. Rev. E **78**, 041603 (2008).
[17] C. M. Aguirre, P. L. Levesque, M. Paillet, F. Lapointe, B. C. St-Antoine, P. Desjardins, and R. Martel, Adv. Mater. **21**, 3087 (2009).
[18] P. L. Levesque, S. S. Sabri, C. M. Aguirre, J. Guillemette, M. Siaj, P. Desjardins, T. Szkopek, and R. Martel, Nano Lett. **11**, 132 (2010).
[19] Y.-J. Yu, Y. Zhao, S. Ryu, L. E. Brus, K. S. Kim, and P. Kim, Nano Lett. **9**, 3430 (2009).
[20] E. H. Hwang and S. Das Sarma, Phys. Rev. B **79**, 165404 (2009).
[21] E. H. Hwang, E. Rossi, and S. Das Sarma, Phys. Rev. B **80**, 235415 (2009).
[22] J. Kong, N. R. Franklin, C. Zhou, M. G. Chapline, S. Peng, K. Cho, and H. Dai, Science **287**, 622 (2000).
[23] O. Leenaerts, B. Partoens, and F. M. Peeters, Phys. Rev. B **77**, 125416 (2008).

Downloaded 08 Jul 2011 to 128.211.161.17. Redistribution subject to AIP license or copyright; see http://apl.aip.org/about/rights_and_permissions